Journal of Optoelectronics and Advanced Materials Vol. 7, No. 1, February 2005, p. 13 - 24

George Nadjakov Lecture

THE IMPACT OF THE ELECTRON SPIN ON CHARGE CARRIER RECOMBINATION – THE EXAMPLE OF AMORPHOUS SILICON

K. Lips*, C. Boehme, T. Ehara

Hahn-Meitner-Institut, Abt. Silizium-Photovoltaik, Kekuléstr. 5, D-12489 Berlin, Germany

The electron spin is generally not considered in recombination processes, since it only marginally influences overall recombination rates. In spite of this, these small changes can be used for the investigation of recombination when spin configurations are manipulated during charge trapping and recombination on time scales much shorter than the lifetime (the coherence time) of the spin. Coherent spin manipulation can be induced by standard pulsed electron spin resonance. The electrical or optical detection of the coherent magnetic resonance does then allow a mapping of the qualitatively different recombination channels, as well as their dynamic behavior. We will review the basic idea of optical spin Rabi oscillation and recombination echo experiments, and discuss the experimental results achieved for the example of amorphous silicon (a-Si:H).

(Received December 9, 2004; accepted January 26, 2005)

Keywords: Recombination, Photoluminescence, a-Si:H, Spin, ESR

1. Introduction

The introduction of pulsed optically and electrically detected magnetic resonance methods (pODMR, pEDMR, respectively) for the investigation of electronic transitions in semiconductor materials has led to new insights and information into the nature of trapping, recombination and transport mechanisms [1-4]. The underlying ideas of these methods is to use pulsed electron spin resonance in order to change the spin states of charge carriers and charge carrier pairs on short timescales (shorter than the coherence times), and to detect changes in the electronic transition rates transiently, at the same time or thereafter. Since the electronic transition rates are detected optically (through luminescence) or electrically (through sample currents), pODMR and pEDMR reach much higher spin sensitivities than conventional pulsed ESR, which is often not applicable to semiconductors (especially low dimensional structures) due to an insufficient absolute spin number. However, the potential of pODMR or pEDMR goes far beyond sensitivity – these combined methods provide unprecedented insights into charge carrier recombination and transport, since they allow the quantitative and qualitative distinction of processes between states with different transitions times, coupling constants, geometric distances and local fields.

In the following, a review is given on how to carry out pODMR on recombination in a disordered semiconductor material. A discussion is presented of what kinds of spin effects can influence recombination, how these effects are observed experimentally and how experimental observations have to be interpreted correctly. We have chosen for this review the historically most prominent example of a disordered semiconductor, hydrogenated amorphous silicon (a-Si:H). This material has been known and subjected to research for more than 30 years [5]. It has a rather complex defect structure with many qualitatively and quantitatively different electronic processes.

In spite of all the research conducted on a-Si:H in the past, there is still much to discover when it comes to the understanding of recombination and transport in this material.

* Corresponding author: lips@hmi.de

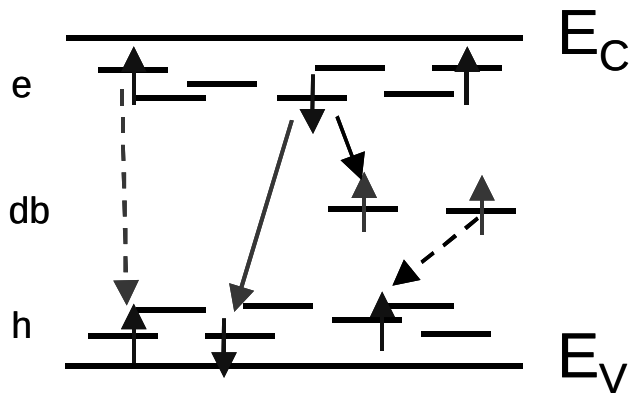

Fig. 1. Principle of spin-dependent recombination in a-Si:H at low temperature between singly occupied tail states (e, h) and dangling bonds (db). Solid lines represent spin allowed and dashed lines spin-forbidden transitions.

2. A brief introduction to PL and ODMR in a-Si:H

Since the discovery of photoluminescence (PL) in a-Si:H by Engemann and Fischer in 1974 [6] many experiments have been carried out to identify the recombination mechanisms. With the number of experiments conducted, the number of models for the explanation of the observations also increased. In a-Si:H, a complex interaction of photogenerated excess charge carriers with a high density of localised states that are distributed over a wide energy range in the forbidden gap exists. This results in a wide distribution of distances between recombining electron-hole pairs and defect states [7-10]. From the study of quadrature frequency-resolved spectroscopy (QFRS) [9, 10], it soon became clear that two peaks in the PL lifetime distribution were observed. These did not correlate with the standard radiative tunnelling model as proposed by Tsang and Street [8]. Stachowitz *et al*. proposed an excitonic recombination model to resolve this discrepancy [10]. Excitonic recombination in the low temperature PL was proposed before by Engemann and Fischer [6] and later by Wilson *et al*. [11] and from various continuous wave (cw) optically detected magnetic resonance (ODMR) studies [12-15]. Cw ODMR is based on the adiabatic manipulation of the spins of recombining electron-hole pairs (e-h), which then change the PL efficiency. It is performed by measuring the PL while the sample is brought into ESR resonance. A disadvantage of this technique is that the interpretation of the spectra becomes very difficult, since often positive and negative signals overlap [16]. In particular, the complex dependence upon experimental conditions such as probing frequency, light intensity, microwave power, and temperature led to very contradictory observations [12-15, 17]. For instance, a resonance at a Landé g value ≈ 4 was observed, which was interpreted as an indication that triplet excitons participate in the PL [15]. The corresponding feature at $g \approx 2$, however, was never satisfactorily identified. One of the problems is the fact that in cw ODMR and time-resolved cw ODMR, moderate to low power microwaves are used, such that the spin population can never be excited coherently. This, however, is necessary to distinguish between recombination channels that stem from the same species but with different coupling strengths to the recombining partners.

3. The nature of spin-dependent recombination

Excess charge carriers in the respective bands of a disordered semiconductor such as a-Si:H get rapidly localised in band tails that are in energetic proximity to the respective band edges. From here, they may recombine with a partner from the other band, or other defects (tail states or dangling bonds (db)). If the charge carriers are located in paramagnetic states prior to recombination

(as sketched in Fig. 1), the recombination probability r will strongly depend on their relative spin orientation. In a homogeneous magnetic field of strength B_0, four different spin configurations exist (↑↑, ↓↓, ↑↓, ↓↑) with non-degenerate Zeeman levels, as shown in Fig. 2. The Zeeman splitting of the four levels is on the order of 10 GHz for $B_0 = 0.35$ T (X-Band ESR). The recombination rate (one should rather call this the trapping rate) from the four different states labelled |1>, |2>, |3>, |4> into the doubly occupied singlet ground state (labelled |S> in Fig. 2) is strongly dependent on the relative spin orientation. In addition, these transition probabilities also depend on the spin-spin interaction between the two spins which are expressed by the exchange coupling constant J and the dipole coupling constant D. The generalised recombination rate can then by calculated as [1]:

$$\begin{aligned} r_1 &= r_T \\ r_2 &= \frac{r_S}{2}\left(1-\frac{J+D}{\Delta}\right)+\frac{r_T}{2}\left(1+\frac{J+D}{\Delta}\right) \\ r_3 &= \frac{r_S}{2}\left(1+\frac{J+D}{\Delta}\right)+\frac{r_T}{2}\left(1-\frac{J+D}{\Delta}\right) \\ r_4 &= r_T \end{aligned} \qquad (1)$$

where r_T denotes the pure triplet and r_S the pure singlet recombination rate and Δ is defined as

$$\Delta = \sqrt{(J+D)^2 + \hbar^2 \Delta\omega^2} \quad . \qquad (2)$$

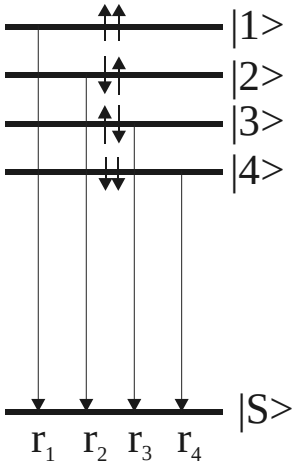

Fig. 2. Sketch of the energy levels of the four different spin configurations that exist for the situation in Fig. 1, with their respective recombination rate coefficients that may be calculated according to Eq. 1.

Here, $\Delta\omega$ is the energy difference between the Lamor frequency $\omega_i = g_i \mu_B B_0/\hbar$ of the two non-interacting spins (g_i: the Lande factor of spin i, μ_B: the Bohr magneton). $\Delta\omega$ may be visualised as the splitting of the two respective lines in the ESR spectrum, and is determined by the two g values. Both, J and D, are determined by the local geometry of the recombining spin pair, e.g. the alignment of the two spins with respect to the direction of the external magnetic field, their charge distribution and their distance. One can distinguish three different regimes of spin-spin interaction strengths as shown in Fig. 3a-c: (a) Absence of spin-spin interaction ($J+D << \hbar\Delta\omega$). This case is valid for distant pair tunnelling recombination, when the average distance between the pair partners is so large that the two spins do not couple. Both spins can be manipulated individually by ESR, and hence two lines at their respective g values with equal intensity will appear in an ODMR spectrum.

Recombination from states $|\uparrow\downarrow>$ and $|\downarrow\uparrow>$ becomes strong (spin allowed) with $r_{2,3} = r_S/2$, and recombination from states |T+> and |T-> becomes weak (spin-forbidden) with $r_{1,4} = r_T$, as can be seen from Eqs. 1 and 2. (b) Intermediate spin-spin interaction ($J+D \approx \hbar\Delta\omega$): with increasing spin coupling, the singlet character of the two middle Zeeman levels in Fig. 3 changes, thereby changing the eigenbase (|2>, |3>). From Eq. 2, one can see that the recombination rate from state |2> is decreased, whereas that from state |3> is enhanced. Note that the pure triplet states are not altered by the change in spin coupling. Also note that the ESR induced transition probability between the pure triplet states and |3> decreases. (c) Large spin-spin interaction ($J+D >> \hbar\Delta\omega$): The singlet character of |2> is further reduced, and for infinite large coupling this will become a pure triplet state (|T0>) whereas |3> becomes a pure singlet state (|S>). For infinite coupling, an ESR transition can only be induced among triplet states that have the same recombination probability r_T (Eq. 1). Hence, ESR can no longer induce a net recombination rate change within the recombining spin pair.

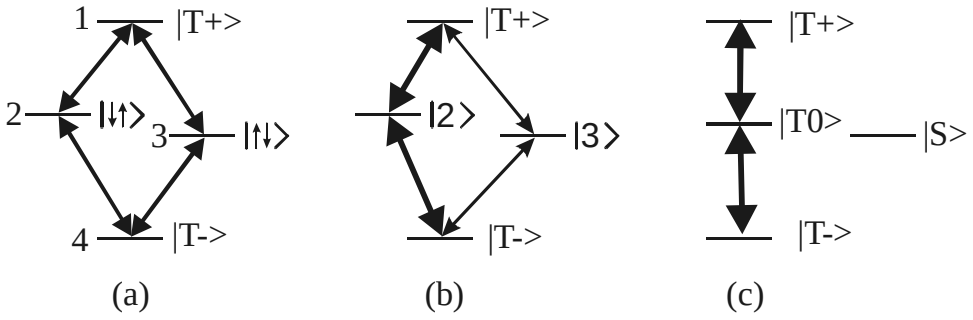

Fig. 3. Qualitative sketch of the four energy levels of the spin pair labelled 1-4 for the case of (a) small (b) medium and (c) large spin-spin interaction, with the respective eigenbase indicated. The thickness of the arrows indicates spin-transition probabilities that can be induced by ESR.

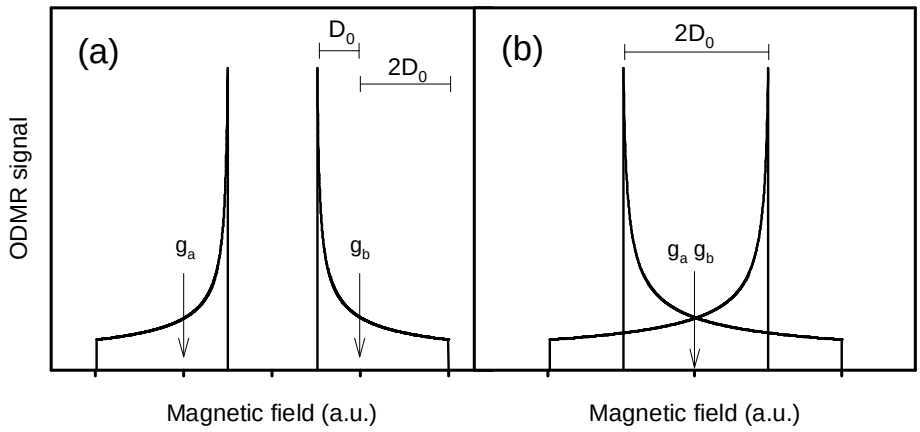

Fig. 4. Change of ODMR spectrum from a two line spectrum of two uncoupled spins a and b (spectra not shown but peak position marked by the arrows) for the case of (a) a small dipolar coupling ($D_0 << \Delta\omega$) and (b) a large dipolar coupling ($D_0 >> \Delta\omega$). Note that the magnetic field in (b) is on a much extended scale, such that the line positions of spin a and b can no longer be separated.

With increasing exchange coupling, the ODMR spectrum will change from a two line spectrum at the respective g values of spins a and b (g_a , g_b) that participate in the recombination event to a one line spectrum at a g value that is the average, $g_a+g_b/2$. When instead dipolar coupling is present, the situation is more complex, since this is an anisotropic interaction. Two spins that

reside at distance r_{ab} with the interspin distance vector $\mathbf{r}_{ab}$ forming an angle Θ with the external magnetic field will experience a local magnetic field D_{ab} that can be calculated [18] as

$$D_{ab} = D_0\left(3\cos^2\Theta - 1\right) = \frac{\mu_B g_a g_b \mu_0}{4\pi\hbar}\frac{1}{r_{ab}^3}\left(3\cos^2\Theta - 1\right). \quad (3)$$

For instance, in a-Si:H it is safe to assume that the recombination partners that are trapped in localised states have their interspin vectors aligned randomly with respect to B_0. In such a situation, the expected ESR or ODMR spectrum can be calculated by integrating over all angles Θ, as performed in Fig. 4. The simple two-line spectrum changes into a complex powder pattern that, depending on the relative strength of the coupling constant D_0 (see Fig 4a and b) may be distributed over a very large range of magnetic field. On the other hand, if such a typical powder pattern is observed in the ODMR spectrum, one is able to reconstruct the interspin distance, an important requisite for the interpretation of the PL in a-Si:H.

3.1 Problems with standard ODMR interpreation

In Fig. 5, a typical ODMR spectrum is shown, as measured using the conventional magnetic field modulation technique. The spectrum was integrated and shows an almost structureless enhancing signal at g = 2.008, as has previously been reported in the literature [16]. For comparison, the expected line positions of the known ESR resonances of electrons (e) and holes (h) trapped in their respective band tails, as well as the dbs, are included in Fig. 5. Changing the measuring parameters leads to changes in the sign of the ODMR signal, and some substructures appear that have been extensively analysed by Cavenett *et al.* [16]. As already pointed out by Cavenett *et al.*, g values can only be determined when a full analysis of the dependence of the spectra on various parameters is performed. To fit the data, however, Cavenett *et al.* use simple lineshapes such as Lorentzians and Gaussians. At first sight this seems appropriate, since the typical structure as predicted for dipolar coupled spin pairs is obviously not identifiable in the ODMR spectrum (compare Figs. 4 and 5). However, in the following we will show that this assumption is wrong. Another critical parameter is the sign of the various ODMR features observed. Usually it is argued that a spin dependent radiative process with thermalized spins is always enhanced under the influence of ESR. However, Boehme and Lips recently showed that depending on the time window where an ODMR or EDMR spectrum is taken both, positive and negative signals can occur [3]. This is due to the fact that any spin dependent process as described by Eq. 1 is associated with at least two, and in most cases even three recombination time constants. Another problem arises from the fact that the well-known g values of the e, h, and db ESR-lines may change due to exchange coupling between the spins. Cavenett and co-workers were fully aware of this problem, but at the time they had no means of proving that exchange coupling is really present in low temperature recombination.

4. The pulsed ODMR technique and its interpretation

The main difference between pODMR and traditional time-resolved ODMR or cw ODMR, as was used before, is that with pODMR all spins are excited coherently and can perform Rabi oscillations. What this means can be best explained for e-h pairs that are trapped in close proximity to each other. Since high generation rates are usually used in ODMR, the e-h pair will form out of different excitation processes (distant pairs). Therefore, the carriers have lost their spin correlation and will be generated in each of the four eigenstates with equal probability, as sketched in Fig. 2. Note that for geminate pairs which stem from the same excitation process, this is not necessarily the case. Since the lifetime of e-h pairs that are generated in a singlet configuration (25% of all generated e-h pairs) is shorter than that of triplets (see Eq. 1), the density of singlet pairs will clearly be lower than that of the triplets under steady state conditions. In other words, the density of e-h pairs trapped in the triplet configuration will be strongly pumped. For the sake of clarity, we will here assume that the density of triplet pairs clearly exceeds that of singlets by a few orders of

magnitude, such that the e-h pairs in a singlet configuration do not need to be considered in the following. Let us furthermore consider only those e-h pairs with spins which are antiparallel to the external magnetic field (↓↓). In terms of their recombination activity, such pairs can not be distinguished from those with both spins pointing upwards (↑↑). Note that all these assumptions are not a requisite for the general idea, but have to be taken into account for theoretical predictions. Here, they are made in order to enhance the clearness of the following explanation.

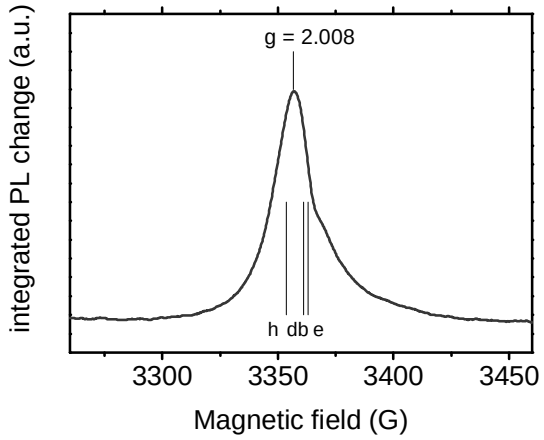

Fig 5. Conventional ODMR spectrum taken at 5K. The positions of the known ESR resonances are indicated.

When we now apply a strong ESR microwave burst that is in resonance with the trapped electrons. Their spins will start to turn away from their down position towards the up position, and then down again. This is called a Rabi oscillation. When a hole spin is weakly coupled to the electron spin, the hole spin will not experience the microwave and its spin will remain unchanged. Therefore, the spin configuration of the e-h pair will oscillate between singlet and triplet configurations. As a consequence, the recombination activity will also oscillate, which can be monitored as an oscillating PL transient. Note that when the microwave burst ends, the spin motion of the electron will also stop, and the spin configuration is frozen until a spontaneous process such as a spin flip (so called spin relaxation), a recombination event or spin scattering occurs. The Rabi frequency, f_{rabi}, is directly proportional to the magnetic field B_1 of the ESR microwave, and to the total spin S. Note that for triplet states, S = 1 and hence f_{rabi} is twice as high as in case of the uncoupled e-h pair which comprises two S = 1/2 particles, where only one spin partner is moved.

For the example of a-Si:H, the interpretation of pODMR data is much more complex than one would anticipate from the simple hand-waving arguments stated above. The complexity arises from the fact that: (i) the g values of the spins are inhomogeneously distributed due to disorder which leads to a distribution of Rabi frequencies; (ii) there is a distribution of the e-h separations and at the generation rates used in our experiment, some of the e-h pairs will be so close together that their mutual coupling cannot be neglected and they have to be treated like excitons with S = 1; (iii) recombination lifetimes of the order of µs have been reported under steady state conditions, and have to be taken into account as a mechanism of coherence loss; (iv) the driving microwave field B_1 can be distorted and may therefore be broadly distributed. We have calculated the expected pODMR transient for different cases, using the basic theory derived for the time-domain of spin dependent recombination [1]. The predicted pODMR transients are plotted in Fig. 6, and were calculated assuming the two extreme cases of weakly and strongly exchange-coupled spin pairs, such as e-h pairs in close proximity. An inhomogeneous g value distribution of about 1 mT was assumed. The transits were calculated assuming typical driving B_1 fields that are used in our experiments for two situations: (Fig. 6a) with strong decoherence (τ_{dec} = 400 ns) for instance due to recombination; (Fig. 6b) a linear distribution of microwave field strengths is assumed that leads to a strong dephasing on a time scale much faster than decoherence (recombination). As becomes obvious from

Fig. 6, Rabi oscillations are predicted in the PL. These are exponentially damped with τ_{dec}. However, note that f_{rabi} is twice as high in the case of strong coupling than in the case of weak coupling. As indicated by the arrows in Fig. 6a, this is simply due to the fact that for weak coupling, both spins can be treated as separate S = 1/2 particles, whereas for strong exchange coupling the spin can no longer be turned individually and the spin pair behaves like one S = 1 particle that is turned at double the frequency. From pODMR or pEDMR transients, three important pieces of information can be drawn: (1) It is possible to discriminate between S = 1/2 particles such as are present in distant pairs and S = 1 particles like excitons, by determining the Rabi frequencies present in the pODMR transients. (2) The coherent spin state of spin pairs can be identified optically or electrically with extremely high sensitivity. This is very important for the spin-based read-out concepts of quantum computers [19]. (3) From the damping of the oscillation, one can immediately determine the decoherence time which in many cases is identical to the recombination lifetime of the spin pair [1]. As shown in Fig. 6b, one has to very carefully consider a possible inhomogeneity of the B_1 field, since this will lead to an extremely broad distribution of Rabi frequencies, producing a strong dephasing of the oscillations. This effect is many orders of magnitude more pronounced than that which the g value inhomogeneities in a-Si:H produce (see Fig 6a). Note that the dephasing of S = 1 is faster than that of S = 1/2 particles. One can distinguish dephasing due to inhomogeneities from decoherence like recombination, by means of a recombination-echo experiment [1, 2, 20]. In such an experiment, the dephased spins can be refocussed by applying a 180° phase shifted microwave pulse which turns the spin in the opposite direction. From the echo decay, the decoherence time can then be determined.

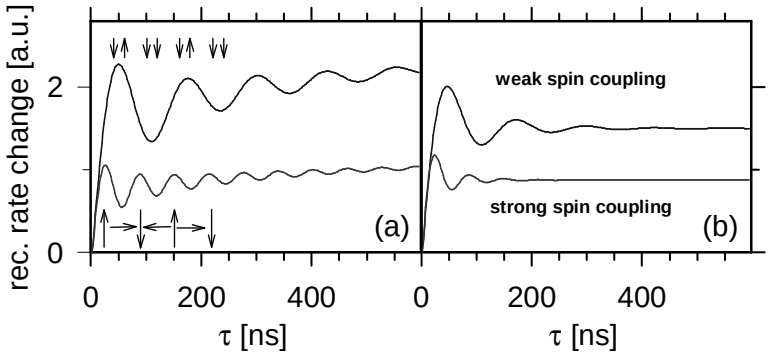

Fig. 6. Calculated recombination rate change induced by a microwave that is in resonance with one of the partners of a spin pair. The spins of the pair are assumed to have weak (upper curve) or strong (lower curve) exchange couplings. An inhomogeneous g factor distribution > 1mT is assumed. (a) with strong decoherence (τ_{dec} = 400 ns) but negligible B_1 distribution, (b) with a constant distribution of B_1 but negligible decoherence. The arrows in (a) represent the spin orientations of the pair at the peaks of the Rabi oscillations. The length of the arrow is proportional to the total spin.

5. Experimental details

The above described pODMR experiment demands that the microwave burst must be sufficiently strong that the spin flip rate is higher than the fastest process that destroys the spin coherence. If this is the case, the spin configuration of the trapped e-h ensemble will be able to perform several oscillations before it looses its phase memory. Typical decoherence times in indirect gap semiconductors (such as silicon) are on the order of a few 100 nanoseconds. Therefore, f_{rabi} should be of the order of 10 - 100 MHz. To accomplish this, microwave powers of the order of kW are needed. Note that in the case of the traditional cw ODMR, only a few mW are available. For the coherent amplification of the 100 mW ESR microwave radiation, a 1kW travelling wave tube amplifier was used, yielding microwave field strengths in the lower mT-range and allowing Rabi frequencies as high as 50 MHz. The pulse length could be varied in steps of 2 ns, and pulse length accuracies were in the ps range. The pODMR experiments were performed using a Bruker Elexsys

580 FT-EPR X-band spectrometer (9.5 GHz) on thin (1 µm) layers of undoped a-Si:H, which were deposited on 1737 Corning glass by plasma-enhanced chemical vapour deposition (PECVD) at the University of Marburg, Germany. Details about the samples can be found in [21]. The samples were previously light soaked. The experiments were carried out at T = 10 K in the pulse cavity, and excess charge carrier generation was performed by the 514 nm line of a cw Ar^+-laser. The laser light was guided by a glass-fibre that was part of a fibre bundle positioned above the a-Si:H sample. The sample and the end of the glass fibre were positioned inside a sealed ESR quartz sample tube of 4 mm diameter. Typical generation rates used in our experiment were $G = 10^{22}$ $cm^{-3}s^{-1}$. The PL signal was collected by the fibre bundle, and was detected without wavelength selection by an InGaAs detector. The laser line was removed by an appropriate cut-off filter. The PL signal was fed into a fast digitizer and analysed according to a procedure previously reported for pEDMR to obtain ns time resolution in the PL transient [1].

6. Experimental results

A pODMR measurement is performed in the following way: A microwave pulse of length τ is applied and induces a coherent change of the spin orientation of those spin pairs that are in ESR resonance. At the end of the pulse, the overall spin configuration will relax back to the steady state condition which existed before the pulse was applied, through incoherent processes such as recombination or spin relaxation [20]. This relaxation transient is recorded with µs time resolution. Then τ is increased by 2 ns and the measurement of the transient is repeated. Plotting the PL intensity chosen at a fixed but otherwise arbitrary time $t_{\mu s}$ after the end of the pulse as a function of τ produces the pODMR plot shown in Fig. 7. Basically, this procedure was shown to fully reconstruct the PL behaviour on a ns time-scale during the application of the microwave pulse, although the time resolution of the set-up is only in the µs range [1].

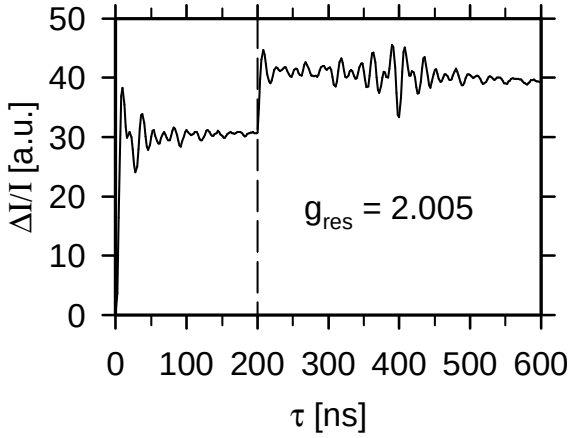

Fig. 7. Experimental pODMR transient of a-Si:H taken at T = 5 K. The magnetic field was chosen such that spins with g values around 2.005 were at resonance. At τ = 200 ns, a 180° phase change was introduced, generating a PL echo at τ = 400 ns.

As one can observe in Fig. 7, the PL intensity initially increases with time, before it starts to oscillate about a constant value. During the first 200 ns in Fig 7, the PL clearly shows an oscillation that contains more than one Rabi frequency. To make sure that these oscillations are not artefacts, we have introduced a 180° phase change of the microwave signal at τ = 200 ns, which forces the spin to rotate in the opposite direction. We observe a nice echo at 2τ = 400 ns, that contains all the features of the transient before the phase change. This clearly indicates that the observed behaviour is solely determined by Rabi oscillations and decoherence.

We have then repeated the experiment in Fig. 7, but varied the position of the external magnetic field between g values of 1.97 and 2.05, thereby bringing the whole set of spin species that

are known to exist in a-Si:H into resonance. For each of the echo transients, a fast Fourier transformation (FFT) was performed and the absolute FFT intensity is plotted in Fig. 8 as a function of the g value. Note the distinct frequencies at about 18 MHz, 25.5 MHz, and 36 MHz. By measuring the Rabi frequency of the db of the a-Si:H sample with standard pulsed ESR under otherwise identical conditions, we have determined f_{rabi} of a S = 1/2 particle to be 18 MHz. Because of this, f_{rabi} is plotted in Fig. 8 in units of 36 MHz. Since this unit represents the Rabi frequency of S = 1 particles, the axis readout can be interpreted as the effective spin that we observe in the pODMR experiment. Note, that the resolution of the FFT plot is limited by the length of the transformed transient, which introduces broadening effects of the features.

In Fig. 8, only those spins show up that participate in PL. We observe an asymmetric island that is produced by centres with S = 1/2 with g values around 2.004-2.005. We can therefore identify these Rabi oscillations as originating from tunnelling recombination of an electron trapped in the conduction band-tail into a weakly coupled neutral db state. From the transient PL signal (not shown here), we find that this is a quenching process.

The second prominent feature is a symmetric, very localised, island at g = 2.008 that stems from a recombination process involving a S = 1 triplet state. No contributions of the excited triplet state of the dbs are found in this resonance, as was reported for µc-Si:H [2, 20] or for P_b centres at the c-Si/SiO_2 interface [22]. Such a spin state typically exists in excitons that may form when an electron and a hole are localised in trap states with very close proximity. In such an exciton, the dipolar coupling is averaged according to Eq. 3, since the spin pair partners will rapidly tumble around each other and all angles are realised within the detection time. For such a case, the g values are also averaged and the resulting value (g = 2.008) is just the average of those of isolated trapped electrons and holes (2.004+2.012/2 = 2.008). To our knowledge, this is the first direct experimental proof that this recombination process originates from excitonic states.

The third prominent feature spreads over a very large range of g values and is associated with f_{rabi} = 25.5 MHz. If one interprets this frequency as an effective spin of the underlying spin pair, we would arrive at $S_{eff} = 0.71 \cdot S_{1/2}$. For strongly dipolar coupled spins, Astashkin and Schweiger [23] have calculated $f_{rabi}^{dip} = 2^{-1/2} \cdot S_{1/2}$ which is in excellent agreement of with our data. Although the total spin of the pair is still S = 1, the effect of dipolar coupling reduces f_{rabi}. The coupling is mediated through dipolar interaction, which could be illustrated as being like a slipping clutch in a car, not fully transforming the total spin into f_{rabi}.

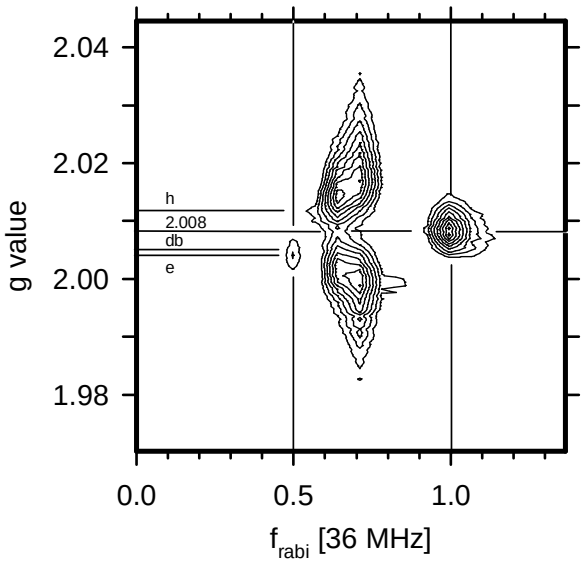

Fig. 8. Contour plot of the Rabi frequency, determined through a FFT of a set of echo traces similar to those in Fig. 7, which were measured as a function of B_0. B_0 is expressed in units of the g value and f_{rabi} in units of the frequency expected for a S = 1 spin pair. The lines indicate the known ESR centres in a-Si:H.

The line shape of this 25.5 MHz feature, determined at f_{rabi} = 25.5 MHz, is plotted in Fig. 9. Here, one can clearly observe a similar line shape to that predicted by the simple dipolar coupling model present in Fig. 4b for the case of strong coupling. The associated average g value can be identified with an e-h pair trapped in their respective tail states. The fact that such a line shape is observed immediately implies that the spins are trapped and do not tumble around each other. We therefore assign this feature to localised e-h pairs. Note, however, that the features are somewhat smeared out in Fig. 9. This is due to the fact that in the case of a-Si:H there is an e-h distance distribution and hence a distribution of dipolar coupling constants D_0. From Fig. 9 and Eq. 3 one can easily estimate the minimal distances of e-h pairs that participate in the PL as r_{min} = 9±1 Å. From the distance between the two peaks in Fig. 9 ($2D_0$), an average distance of r_{av} = 16±2 Å is estimated. Since we do not observe any features between the exciton and the dipolar coupled e-h pairs, we believe that once the distance of an e-h pair is below about 9 Å, an exciton is formed in a-Si:H. To our surprise, we could not detect a major difference in the coherence time between the exciton and the distant e-h pairs. In both cases, we observe about 2 µs. At present we have no explanation for this, it may suggest though that the coherence times of these centres are not limited by recombination but by spin relaxation.

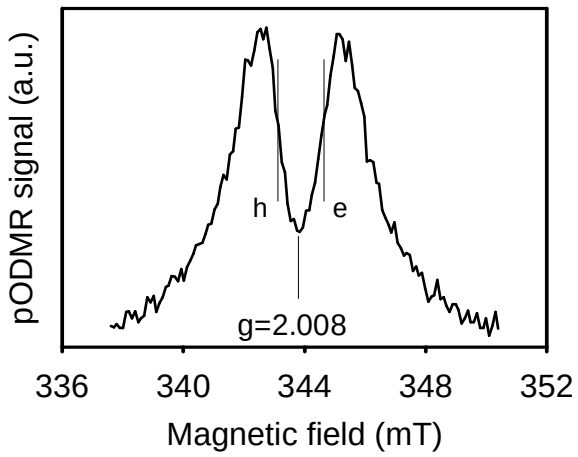

Fig 9. Spectrum extracted from Fig. 8 at f_{rabi} = 25.5 MHz.
Markers of the e and h resonances are shown

We have tried to simulate the observed dipolar feature of Fig. 9 with Eq. 3, assuming various distributions of distances. However, we failed to get good agreement. Note that Eq. 3 is only valid if the charge distribution has axial symmetry along the connection line between the e-h pair. This seems clearly not to be the case for the e-h pair in a-Si:H. Thus, the wavefunctions of the tail states do not seem to have the symmetric spherical s-like wave function that has often been assumed in the literature.

7. Discussion

From the experimental results outlined above, we can unambiguously identify three distinctly different recombination processes in the low temperature PL of a-Si:H. Recombination through the excited triplet states of the dbs (known as the direct capture process) or P_b centres at the c-Si/SiO_2 interface is not observed. This might be related to the low density of dbs in a-Si:H, as well as to the low mobility of all charge carriers. Using the generation rate of our experiment ($G = 10^{22}$ $cm^{-3}s^{-1}$), the average distance between e-h pairs when randomly distributed among tail states can be estimated to less than 300 Å, if an average lifetime of about 1µs is assumed. In this regime, distant pair kinetics clearly prevails [9, 10]. This implies that the spin memory of the recombining e-h pairs is lost, and the four possible Zeeman levels are populated with equal

probability. As a consequence, those Zeeman levels with the lowest recombination probability are pumped, as explained in section 3. Turning the spin of this sub-ensemble will lead to an enhancement of the recombination rate. Since we observe an initial enhancement of the PL for both S = 1 features, we assign both processes to a radiative recombination channel. Note that our time resolution is orders of magnitude better than that in conventional cw ODMR. Nevertheless, one has to be very careful about such an interpretation of the sign of an ODMR signal, since it is dramatically based on the assumption that all spin states are equally generated and that no complex shunting of recombination occurs, as is present with strongly competing channels. In such a case, enhancing and quenching have to be interpreted in just the opposite way.

From the symmetry of the dipolar features around the ESR resonance positions of e and h (Fig. 9), we conclude that this signal arises from trapped e and h pairs in their respective tails, with the distance between the constituents of the pair being larger than about 9 Å. If the e-h pairs are trapped in closer proximity, an excitonic state with large exchange coupling will form.

The fact that both S = 1 channels appear with about the same time constant of a few µs in our pODMR experiment is at present not fully understood. Moreover, it would be very interesting to know the lifetime of the singlet exciton and the singlet state of the dipolar coupled e-h pairs. From Fig. 3, it becomes clear that in the case of strong coupling, no ESR transition between the triplet states and the singlet state is possible. Hence, the singlet configuration cannot be manipulated by ESR, and hence no information can be obtained.

The process involving the db at about g = 2.0050 is the well known non-radiative tunnelling recombination between a conduction ban tail state and a neutral db. Since no dipolar or exchange coupling is present, this process involves a tail electron trapped at a large distance from a neutral db. Therefore, both spin-pair partners can be manipulated individually, and the feature in Fig. 8 has the signature of S = 1/2.

8. Conclusions and outlook

We have given a comprehensive overview of spin dependent processes that affect the low temperature PL of a-Si:H. It was demonstrated that ODMR techniques have the sensitivity and selectivity to distinguish different recombination channels very accurately. It is the coherent manipulation of the spin ensemble that enables one to extract valuable information about the recombination mechanism, by observing this collective spin motion as Rabi oscillations in the PL. The pODMR technique allows one to separate different spin processes through their characteristic Rabi frequency.

We have clearly identified three distinctly different recombination mechanism, namely (i) non-radiative tunnelling of band-tail electrons to neutral dbs; (ii) radiative tunneling between dipolar coupled distant band-tail electrons and holes that are separated by more than 9 Å; (iii) e-h pairs that form an excitonic state. We interpret the 9 Å limit, below which hardly any dipolar coupled pairs are detected, as the localisation length of the excitonic state. Thus, the origin of excitons in a-Si:H appears to be conduction and valence tail states which are located at a proximity of less then 9 Å. A direct capture process at dbs, as observed in µc-Si:H and at P_b centres at the c-Si/SiO_2 interface, is not observed at T = 10 K.

One of the most surprising results was that we now have access to the charge separation of e-h pairs during recombination. It should be most interesting to study this in more detail by analysing the pODMR time dependence of the spectra and studying this as a function of the generation rate. For this, however, an appropriate distance (and lifetime) distribution of the e-h pairs has to be found which is able to explain the observed features in the pODMR spectra.

Acknowledgement

The authors would like to thank Prof. W. Fuhs for stimulating discussions and for enabling us to perform such complex experiments at the HMI. T. Ehara gratefully acknowledges funding by the Ishinomaki Senshu University (Japan) that allowed him to visit the HMI for one year. We also

highly appreciate the helping hand of K. Petter with a lot of experimental problems. We are indebted to H. Mell (formerly Universität Marburg, Germany) and K. Pierz (PTB, Braunschweig) for supplying the a-Si:H samples.

References

[1] C. Boehme, K. Lips, Phys. Rev. B **68**, 245105 (2003).
[2] C. Boehme, K. Lips, Phys. Rev. Lett. **91**, 246603 (2003).
[3] C. Boehme, K. Lips, phys. stat. sol. (c) **1**, 1255 (2004).
[4] C. Boehme, K. Lips, J. Non-Crys. Solids **338-340**, 434 (2004).
[5] R. A. Street, Hydrogenated Amorphous Silicon (Cambridge University Press, Cambridge, 1991).
[6] D. Engemann, R. Fischer, in Amorphous and Liquid Semiconductors, ed. J. Stuke and W. Brenig (Taylor and Francis, London, 1974), p. 947.
[7] B. I. Shklovskii, H. Fritzsche, S.D. Baranovskii, Phys. Rev. Lett. **62**, 2989 (1989).
[8] C. Tsang, R.A. Street, Phys. Rev. B **19**, 3027 (1979).
[9] S. Ambros, R. Carius, H. Wagner, J. Non-Cryst. Solids **137-138**, 555 (1991).
[10] R. Stachowitz, M. Schubert, W. Fuhs, J. Non-Cryst. Solids **227 - 230**, 190 (1998).
[11] B. A. Wilson, P. Hu, J. P. Harbison, T. M. Jedju, Phys. Rev. Lett. **50**, 1490 (1983).
[12] S. Depinna, B. C. Cavenett, I. G. Austin, T. M. Searle, M. J. Thompson, J. Allison, P. G. Le Comber, Phil. Mag. B **46**, 473 (1982).
[13] S. Depinna, B. C. Cavenett, I. G. Austin, T. M. Searle, Phil. Mag. B **46**, 501 (1982).
[14] F. Boulitrop, Phys. Rev. B **28**, 6192 (1983).
[15] J. Morigaki, J. Non-Cryst. Solids **77-78**, 583 (1985).
[16] B. C. Cavenett, S. P. Depinna, I. G. Austin, T. M. Searle, Phil. Mag. B **48**, 169 (1983).
[17] D. K. Biegelsen, J. C. Knights, R. A. Street, C. Tsang, R. M. White, Phil. Mag. B **37**, 477 (1978).
[18] A. Weber, O. Schiemann, B. Bode, T.F. Prisner, J. Magnetic Resonance **157**, 277 (2002).
[19] C. Boehme, K. Lips, phys. stat. sol. (b) **233**, 427 (2002).
[20] K. Lips, C. Boehme, J. of Material Science - Materials in Electronics **14**, 635 (2003).
[21] K. Pierz, W. Fuhs, H. Mell, Phil. Mag. B **63**, 123 (1991).
[22] F. Friedrich, C. Boehme, K. Lips, to be published.
[23] A. V. Astashkin, A. Schweiger, Chem. Phys. Lett. **174**, 595 (1990).